ELSEVIER

Journal of Power Sources 84 (1999) 12–23

JOURNAL OF POWER SOURCES

www.elsevier.com/locate/jpowsour

Synthesis and characterization of polyether urethane acrylate–$LiCF_3SO_3$-based polymer electrolytes by UV-curing in lithium batteries

Cheon-Soo Kim, Bo-Hyun Kim, Keon Kim *

Department of Chemistry, Korea University, 1 Anam-dong, Sungbuk-ku, Seoul 136-701, South Korea

Received 16 October 1998; accepted 15 November 1998

Abstract

The prepolymers of polyether urethane acrylate (PEUA) were synthesized from polyether polyol (polyethylene glycol (PEG) or polypropylene glycol (PPG)), diisocyanate (hexamethylene diisocyanate (HMDI) or toluene 2,4-diisocyanate (TDI)), and the caprolactone-modified hydroxyethyl acrylate (FA2D) using the catalyst (dibutyltin dilaurate (DBTDL)) by stepwise addition reaction. Lithium triflate ($LiCF_3SO_3$) was dissolved in PEUA prepolymers, and plasticizer (propylene carbonate (PC)) was added into prepolymer and salt mixtures. Then photoinitiator (Irgacure 184) was also dissolved in the mixtures. Thin films were prepared by casting on the glass plate, and then by curing the plasticized prepolymer and salt mixtures under UV radiation. Electrochemical and electrical properties of PEUA–$LiCF_3SO_3$-based polymer electrolytes were evaluated and discussed to be used in lithium batteries.

Keywords: Urethane acrylate; UV-curing; Polymer electrolytes; Lithium batteries

1. Introduction

Much effort in the investigation and development of new ionically conducting polymers, classified as polymer electrolytes, is currently being devoted to developing advanced electrochemical storage systems [1] because lithium polymer batteries are very promising systems in terms of energy density and power density [2] and also because polymer electrolytes offer many advantages; for example, easiness of fabrication in form of thin film, high electrochemical and chemical stability, and high lithium transference number [3].

Today, special interest is focused on polymer systems having high ionic conductivity at ambient and sub-ambient temperatures, since they may find unique applications, such as separators in high-power rechargeable lithium battery. The two important variables in the conductivity of polymer are the degree of crystallinity and the glass transition temperature [4]. Until now, among the most promising examples are gel-type electrolytes obtained by the immobilization of liquid solutions (e.g., propylene carbonate–ethylene carbonate, PC-EC mixture solvents) of lithium salts in a polymer matrix, for example, poly(acrylonitrile) PAN [5,6] or poly(methylmethacrylate) PMMA matrix [6,7]. In order to improve mechanical properties of gel polymer electrolytes, components, which can be cross-linked, and/or thermoset, are added to the gel electrolyte formation. Crosslinked polymer networks prepared using radiation curing have received considerable attention in recent years.

The UV curing process offers several advantages over conventional processes in the coating industry. These benefits include high speed of processing and high-energy efficiency since the polymerization is carried out at room temperature. The most important UV-curables are based on urethane–acrylate (UA) oligomers. The isocyanate-PEG cross-linking idea came from Le Nest et al. [8] and the plasticized polyether urethane electrolytes based on PEG-lithium salt complexes were characterized by Borghini et al. [9]. Systematic study of urethane–acrylate UV-curables carried out by Stuart L. Cooper's laboratory [10]. Typical prepolymers of this family are made by reacting a low

* Corresponding author. Tel.: +82-2-3290-3128; Fax: +82-2-928-7387

0378-7753/99/$ - see front matter
PII: S0378-7753(99)00269-4

molecular weight polyether diol with an excess of diisocyanate. The remaining diisocyanate functionalities are then tipped with small acrylate-containing species to give long molecules tipped with acrylic functionality at each end. This prepolymer is diluted by small molecules containing vinyl group or solvent and then cross-linked in a free radical type polymerization by exposing to UV radiation in the presence of a photoinitiator.

The polyol in the PEUA is called the soft segment because of its low glass transition temperature and hence its high degree of flexibility. An increase in the soft segment molecular weight (thereby also increasing the weight fraction of the soft segment) causes the prepolymer to have higher viscosity. The cured polymer has better phase separation of the hard and soft segments. The hard segment (the isocyanate part of the polymer segment, which has very little flexibility) and the soft segment affect the properties of the UV-curable to a large extent. In general, a well-phase-separated material has better mechanical properties than a poorly phase-separated material. Although PEUA matrix has also considerable merit because these offer excellent toughness, chemical resistance, flexibility, and adhesion to difficult substrates and also because modifications of the backbone of PEUA, such as variations in chain length and other functional parameters, will result in a variety of mechanical properties [11], their basic electrochemical properties have not been yet fully understood.

In the present paper, basic electrochemical properties were studied and discussed for PEUA–$LiCF_3SO_3$-based polymer electrolytes in terms of the conductivity, the lithium transference number, the electrochemical stability

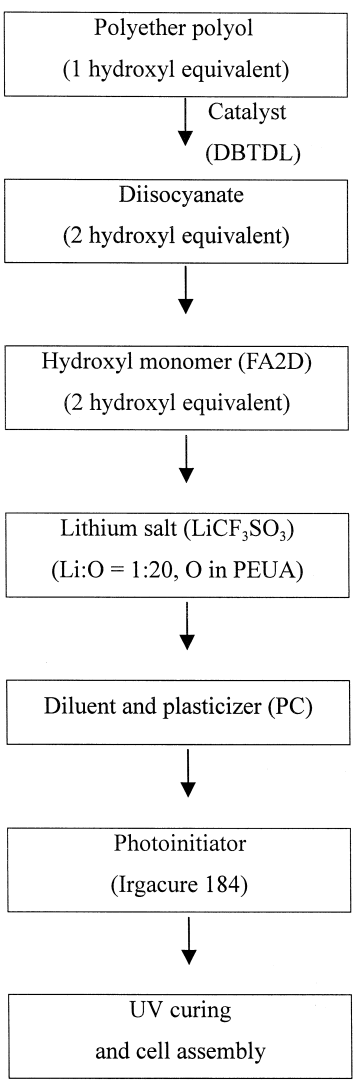

Fig. 1. The synthesis procedure for PEUA–$LiCF_3SO_3$-based polymer electrolytes.

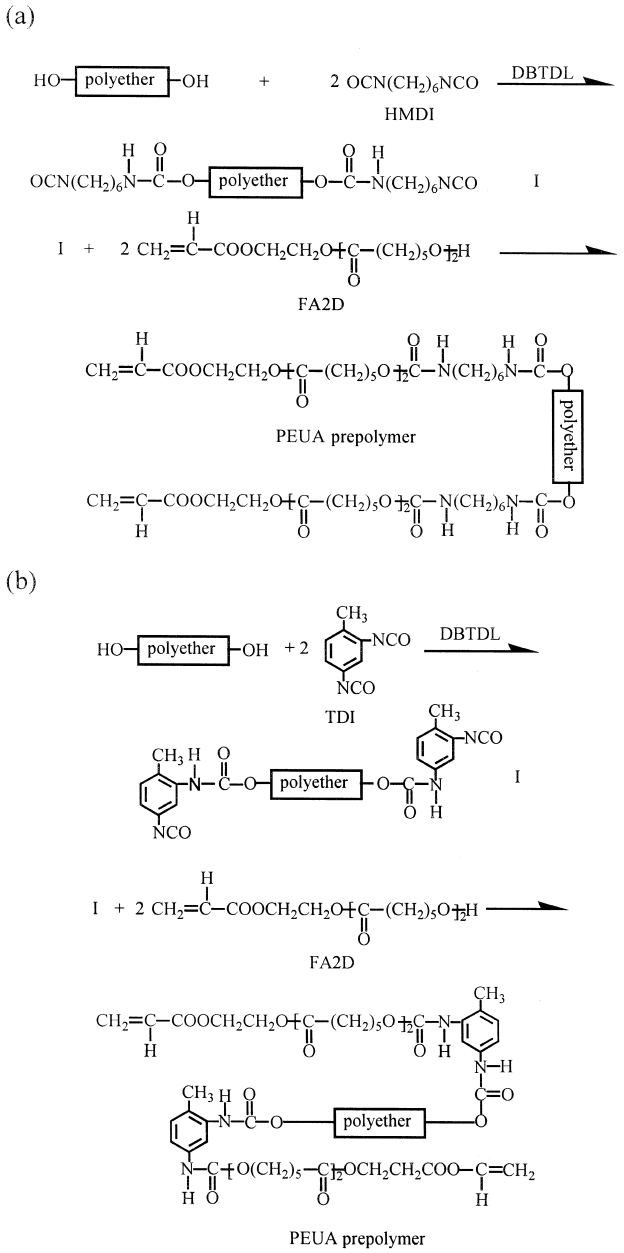

Fig. 2. The preparation of PEUA with (a) HMDI and with (b) TDI.

Table 1
Molar composition of PEUA polymer networks and PEUA–$LiCF_3SO_3$-based polymer electrolytes

Sample	Composition
S1	PEG 200 5/HMDI 10/FA2D 10
S2	PEG 200 5/TDI 10/FA2D 10
S3	PEG 400 5/HMDI 10/FA2D 10
S4	PEG 400 5/TDI 10/FA2D 10
S5	PPG1000 5/HMDI 10/FA2D 10
S6	PPG2000 5/HMDI 10/FA2D 10
S5-a	PPG1000 5/HMDI 10/FA2D 10/$LiCF_3SO_3$ 9.48
S5-b	PPG1000 5/HMDI 10/FA2D 10/PC 85.55
S5-c	PPG1000 5/HMDI 10/FA2D 10
P1	PEG 200 10/HMDI 20/FA2D 20/PC 78.11/$LiCF_3SO_3$ 11.89
P2	PEG 200 10/TDI 20/FA2D 20/PC 78.11/$LiCF_3SO_3$ 11.89
P3	PEG 400 10/HMDI 20/FA2D 20/PC 75.84/$LiCF_3SO_3$ 14.16
P4	PEG 400 10/TDI 20/FA2D 20/PC 75.84/$LiCF_3SO_3$ 14.16
P5	PPG1000 5/HMDI 10/FA2D 10/PC 85.55/$LiCF_3SO_3$ 9.48
P6	PPG2000 5/HMDI 10/FA2D 10/PC 81.47/$LiCF_3SO_3$ 13.53

window and the phenomena occurring at the interface between these thin films and the lithium metal electrode.

2. Experimental

2.1. Materials

Poly(ethylene glycol) (PEG) [Mw 200, 400 $H(OCH_2CH_2)_nOH$, Aldrich] and poly(propylene glycol) (PPG) [Mw 1000, 2000 $H[OCH(CH_3)CH_2]_nOH$, Aldrich] were dried at 30°C and at 80°C under vacuum for 7 days, respectively. Lithium triflate ($LiCF_3SO_3$) (96%, Aldrich) was dried under vacuum for 48 h at 120°C. Propylene carbonate (PC) (99%, Aldrich), hexamethylene diisocynate (HMDI) (95% Wako) and toluene diisocynate (TDI) (98% Junsei Chemical) were purified by distillation under reduced pressure. The commercial caprolactone-modified hydroxyethyl acrylate (FA2D) [Mw 344 $CH_2CHCOOCH_2CH_2O(CO(CH_2)_5O)_2H$] was purchased from Daicel Chemical Industries and dried under vacuum for 36 h at 40°C.

2.2. Polymer electrolyte preparation

Polymer electrolytes were prepared by the following three-step procedure. In the first step, one equivalent of PEG was reacted with two equivalents of diisocyanate for

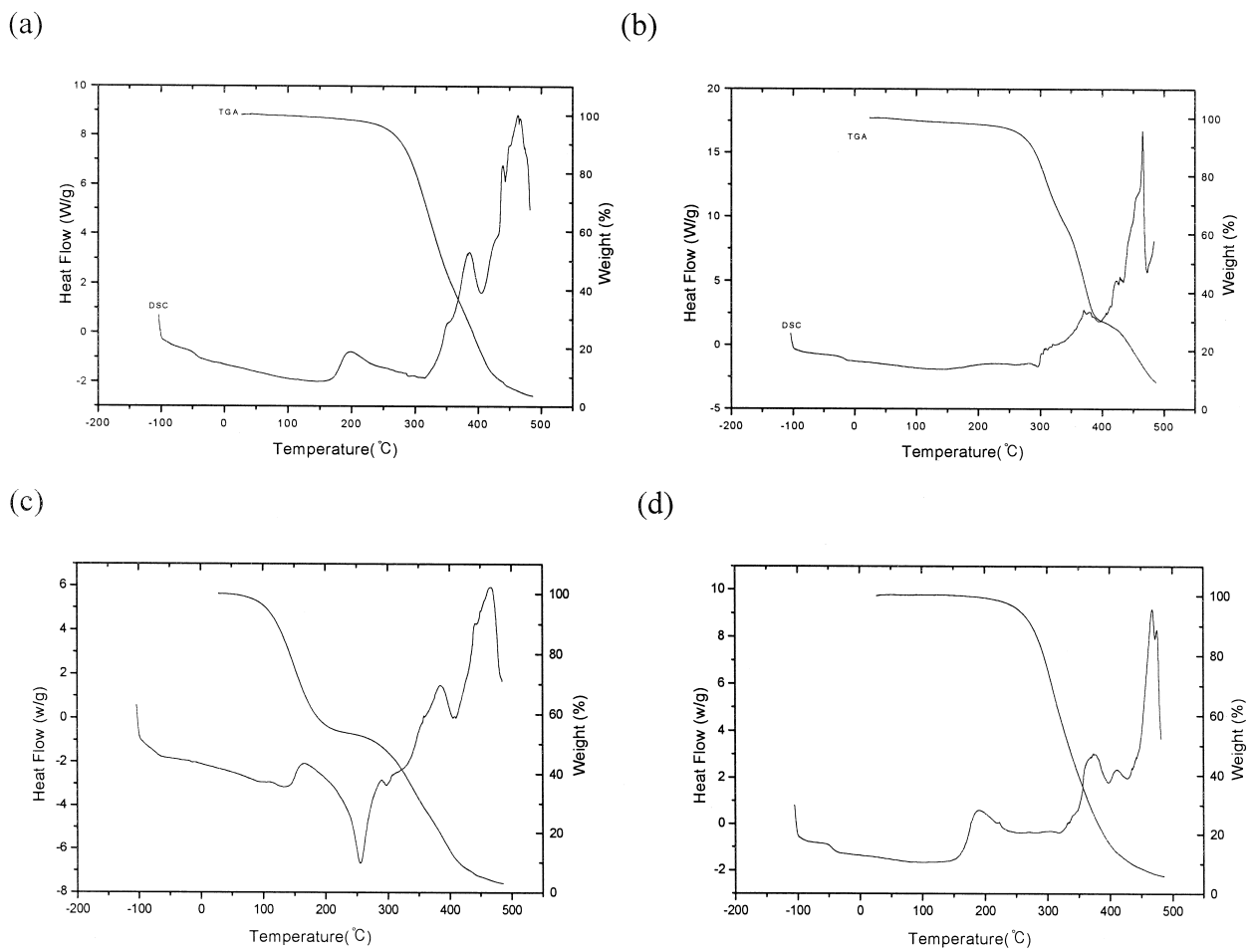

Fig. 3. DSC and TGA thermograms of (a) S5 (PPG1000 5/HMDI 10/FA2D 10), (b) S5-a (PPG1000 5/HMDI 10/FA2D 10/$LiCF_3SO_3$ 9.48), (c) S5-b (PPG1000 5/HMDI 10/FA2D 10/PC 85.55) and (d) S5-c (amorphous S5; PPG1000 5/HMDI 10/FA2D 10).

1 h. Temperature was maintained at 60–70°C. In the second step, isocyanate-capped adduct was reacted with two equivalents of an unsaturated FA2D at 60–70°C for 30 min and then at 80–90°C until the −NCO level is undetectable in FT-IR. Substituting FA2D results in the corresponding PEUA prepolymer. The OH/NCO ratio was stoichiometric. In the final step, the prepolymer was cooled to ~40°C. $LiCF_3SO_3$ (1:20 mole ratio (Li:O in the backbone of PEUA prepolymer)) was directly dissolved under stirring. The prepolymer-salt mixture was diluted by PC and then photoinitiator (Irgacure 184) was dissolved.

The diluted prepolymer–salt mixture was cast on the glass plate. It was stored in a translucent polyethylene (PE) box filled with argon. PE box was transferred to portable UV-curing apparatus in which medium pressure mercury arc lamp (300 W/in.) was used. Mechanically stable freestanding thin film of polymer electrolyte was prepared by curing for 30 s under UV radiation. Fig. 1 shows the procedure for PEUA–$LiCF_3SO_3$-based polymer electrolytes. Fig. 2 shows the preparation of PEUA using HMDI and TDI, respectively. All steps of polymer electrolyte preparation and cell assembly were carried out in a glovebox maintained under argon atmosphere except UV-curing process for which sample was in PE box filled with argon. Table 1 shows molar composition of nine PEUA polymer networks and six PEUA–$LiCF_3SO_3$-based polymer electrolytes selected in this study.

2.3. Thermal analysis

Thermal properties were measured using a differential scanning calorimeter (DSC) and a thermogravimetric analyzer (TGA). DSC data were obtained between −100 and 500°C using a Dupont DSC 2010 under argon atmosphere. Approximately 3–10 mg samples were quenched from room temperature to −100°C by liquid nitrogen. DSC data scannings were carried out at the heating rate of 10°C/min. TGA data were obtained between 25°C and 500°C at the rate of 10°C/min using a Dupont TGA 2050 under argon atmosphere.

2.4. X-ray analysis

X-ray diffraction measurements were made for PEUA–$LiCF_3SO_3$-based polymer electrolyte films to examine the

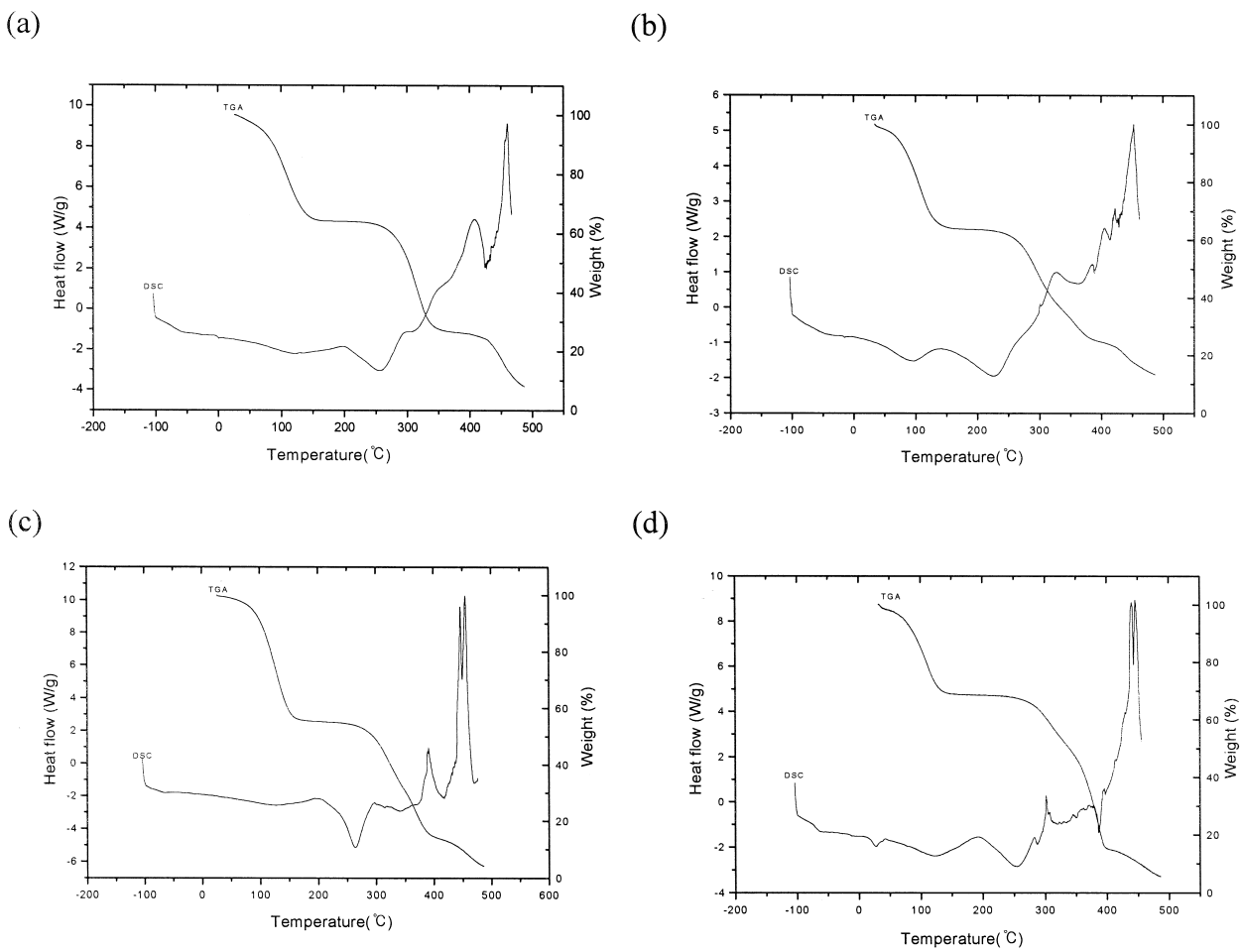

Fig. 4. DSC and TGA thermograms of (a) P1 (PEG 200 10/HMDI 20/FA2D 20/PC 78.11/$LiCF_3SO_3$ 11.89), (b) P2 (PEG 200 10/TDI 20/FA2D 20/PC 78.11/$LiCF_3SO_3$ 11.89), (c) P5 PPG1000 5/HMDI 10/FA2D 10/PC 85.55/$LiCF_3SO_3$ 9.48) and (d) P6 (PPG2000 5/HMDI 10/FA2D 10/PC 81.47/$LiCF_3SO_3$ 13.53).

Table 2
DSC and TGA results of PEUA polymer networks and PEUA–$LiCF_3SO_3$-based polymer electrolytes

Sample	T_g (°C)	T_m (°C)	ΔH_m (J/g)	Decomposition temperature (°C)
S1	−24.9	88.1	14.8	215.0
S2	18.2	–	–	211.3
S3	−49.8	89.0	15.6	196.5
S4	0.7			207.6
S5	−43.3	–	–	197.8
S6	−57.6	–	–	183.2
S5-a	−17.4	–	–	219.7
S5-b	−70.8	–	–	229.9
S5-c	−42.5	–	–	191.2
P1	−66.2	–	–	219.7
P2	−59.3	–	–	207.5
P3	−67.2	–	–	221.8
P4	−53.1	–	–	229.3
P5	−75.2	–	–	197.9
P6	−68.7	–	–	211.0

nature of crystallinity with respect to PC- and $LiCF_3SO_3$-free PEUA polymer network. X-ray diffraction patterns were measured with a Philips X'Pert MPD X-ray diffractometer using a Cu-K_α ray.

2.5. Impedance measurements

Cells for measuring the ionic conductivity were prepared by sandwiching the polymer electrolyte (diameter 15 mm) between two stainless steel (SS 304) electrodes (diameter 23 mm). Ionic conductivity was measured for temperatures ranging from 25°C to 75°C. A potential difference of 5 mV was applied to the sample for frequencies ranging from 100 Hz to 4 MHz.

Cells for investigating the stability of the lithium–PEUA-based polymer electrolyte interface were prepared by sandwiching the polymer electrolyte between two lithium electrodes (diameter 15 mm) made by cold-pressing lithium foil onto stainless steel disks (SS 304, diameter 23 mm). Cells for measuring compatibility with the electrode materials were stored under open circuit conditions at ambient temperature and tested at 25°C. The potential difference of 5 mV was applied to the sample for frequencies ranging 4 MHz to 0.1 Hz. Compatibility was determined from the interfacial impedance obtained from the value of Z' at the minimum of $-jZ''$ at low frequency in Nyquest plot.

Both ionic conductivity of the polymer films and interface phenomena were measured using ZAHNER IM6 model impedance analyzer controlled by THALES software and connected with IBM compatible personal computer. Cells were placed in a temperature-controlled thermostat (temperature accuracy: ±1°C). Each sample was equilibrated at the experimental temperature for 1 h before measurement.

2.6. Cyclic voltammetry

One of important parameters for the characterization of any electrolyte is the extent of its electrochemical stability window. It was evaluated with cell featuring a stainless

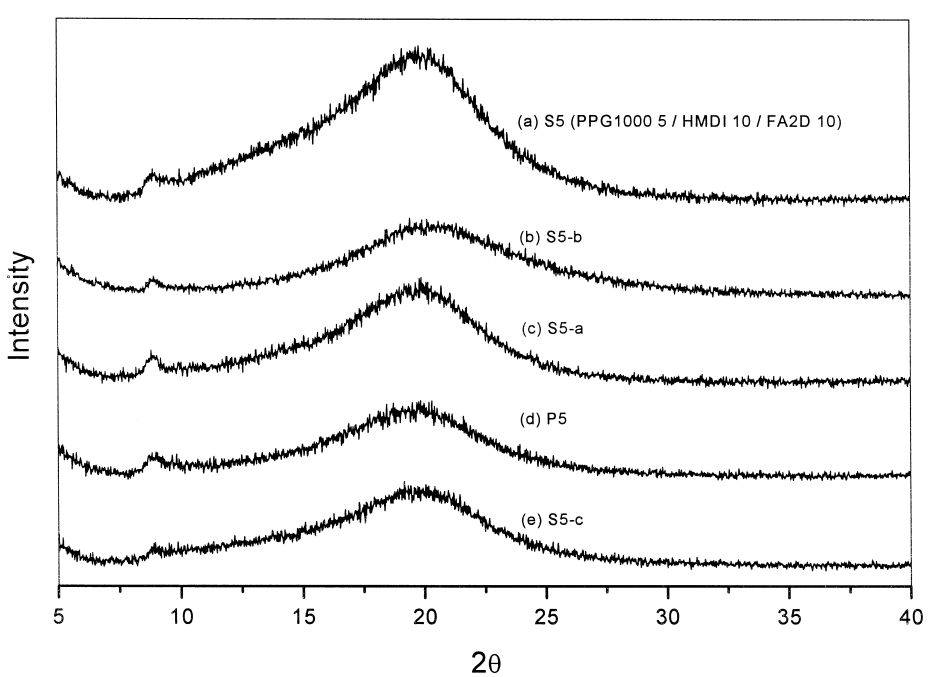

Fig. 5. X-ray diffraction data for (a) S5 (PPG1000 5/HMDI 10/FA2D 10), (b) S5-b (PPG1000 5/HMDI 10/FA2D 10/PC 85.55), (c) S5-a (PPG1000 5/HMDI 10/FA2D 10/$LiCF_3SO_3$ 9.48) (d), P5 (PPG1000 5/HMDI 10/FA2D 10/PC 85.55/$LiCF_3SO_3$ 9.48) and (e) S5-c (amorphous S5; PPG1000 5/HMDI 10/FA2D 10).

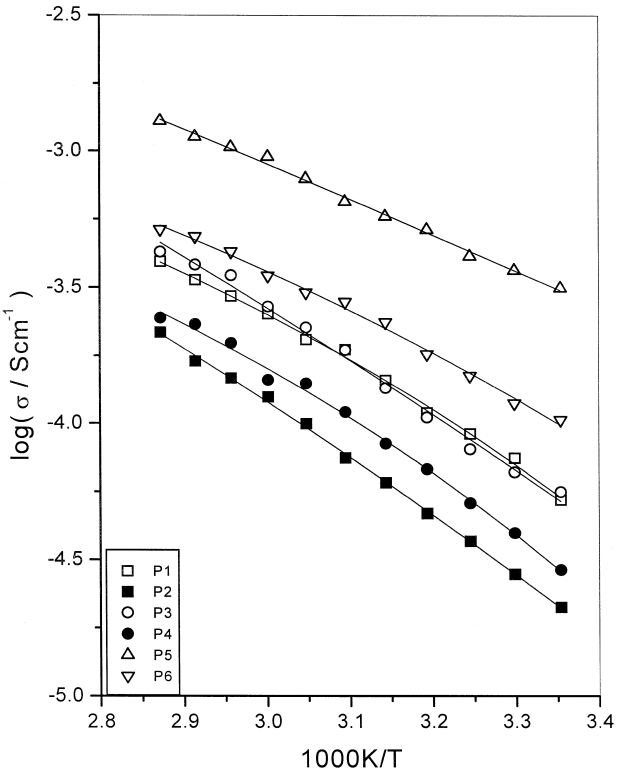

Fig. 6. Ionic conductivity as a function of reciprocal temperature for PEUA–$LiCF_3SO_3$-based polymer electrolytes.

steel (SS304) working electrode and lithium counter and reference electrode by linear sweep voltammetry at 25°C. Electrochemical stability windows and cyclic voltammograms were obtained by means of ZAHNER (IM6 model) potentiostat mode controlled by THALES software.

2.7. Lithium transference number

The Bruce and Vincent method involving the steady-state current (I_s) and the initial current (I_o) has been used the most widely until now to evaluate the transference phenomena of polymer electrolytes [12]. This method consists of measuring by ac impedance the resistance of a symmetrical Li/polymer electrolyte/Li cell and by dc chronoamperometry the current across the same cell polarized by a dc voltage pulse, V and gives the ideal cationic transport number. The measurements are taken at the initial time of the applied dc voltage pulse ($t = t_0$, $R = R_0$, $I = I_0$) and under steady conditions ($t = t_s$, $R = R_s$, $I = I_s$). By using these values, the lithium transference number is given by the expression

$$t_{Li^+} = \frac{I_s(V - I_0 R_0)}{I_0(V - I_s R_s)} \quad (1)$$

where V is the value of the dc voltage pulse applied to the cell for the chronoamperometric analysis (in the case of this work $V = 10$ mV).

3. Results and discussion

3.1. Thermal analysis

Fig. 3 shows the profiles of DSC and TGA thermograms of the S5, salt (S5-a) or PC (S5-b) mixture with S5 and amorphous S5 (S5-c). The molar compositions of S5 series were shown in Table 1. Without PC and $LiCF_3SO_3$, six S series have the same molar composition as six P series. S5-a and S5-b were made by mixing $LiCF_3SO_3$ or PC with S5 homogeneously. Amorphous S5-c was made by quenching S5 at 200°C using the liquid nitrogen. With the incorporation of $LiCF_3SO_3$ in S5, T_g of S5-a was higher than that of S5 alone while T_g of S5-b was lower than that of S5. The increase in T_g for S5-a was due to making the partial complex between Li^+ and oxygen or nitrogen in PEUA. Since the addition of a plasticizing solvent to S5 lowered S5's T_g, T_g for S5-b was decreased.

Fig. 4 shows the DSC and TGA thermograms of four PEUA–$LiCF_3SO_3$-based polymer electrolytes. From TGA, we can say that PC was vaporized from polymer electrolyte between 25°C and 150°C. T_g of P sample is lower than that of S sample. This result shows the same trend as S5 series. As PC plasticized S series so well, T_g's of the samples were mostly effected by the addition of PC. The T_g's of P series were changed from -75.2°C to -53.1°C and decomposition temperatures were about 200°C. T_g's of polymer electrolytes with HMDI were lower than those of polymer electrolytes with TDI as we compared P1 and P3 with P2 and P4. From DSC and TGA thermograms, thermal stabilities of PEUA polymer networks were summarized in Table 2.

3.2. X-ray analysis

Fig. 5 shows X-ray diffraction data for PC- and $LiCF_3SO_3$-free S5 polymer network and S5 series at room temperature. PC- and $LiCF_3SO_3$-free S5 has about 30% crystallinity and S5-a with $LiCF_3SO_3$ about 10% crystallinity while S5 series with PC or both have amorphous phases. This means that the incorporation of $LiCF_3SO_3$ and/or PC with PEUA decreases the crystallinity of PEUA and the effect of PC for reducing the crystallinity was higher than that of $LiCF_3SO_3$.

Table 3
VTF fitting parameters for PEUA–$LiCF_3SO_3$-based polymer electrolytes

Sample	A_σ (μ SK$^{1/2}$/cm)	E_a/k_B (K)	T_0 (K)
P1	0.6	688.4	191.7
P2	29.4	2096.4	112.7
P3	79.4	2295.7	96.7
P4	0.4	675.4	198.6
P5	74.7	2516.4	34.6
P6	0.8	752.7	175.1

Table 4
Electrochemical properties of PEUA–$LiCF_3SO_3$-based polymer electrolytes at 25°C

Sample	Ionic conductivity (S cm^{-1})	Transference number	Decomposition voltage (V) vs. Li
P1	5.2×10^{-5}	0.3	4.1
P2	2.1×10^{-5}	0.4	4.0
P3	5.4×10^{-5}	0.4	4.3
P4	2.9×10^{-5}	0.5	4.8
P5	3.1×10^{-4}	0.5	4.2
P6	1.0×10^{-4}	0.3	4.6

3.3. Impedance

3.3.1. Conductivity

The conductivity (σ) was determined from the bulk resistance (R_b) which was obtained from the value of Z' at the minimum of $-jZ''$ at the high-frequency in the complex impedance plot (Nyquest) [13] where

$$\sigma = \frac{4a}{\pi d^2 R_b}. \quad (2)$$

Here, a is the electrolyte thickness and d is the electrode diameter. Fig. 6 shows ionic conductivity as a function of reciprocal temperature for PEUA–$LiCF_3SO_3$-based polymer electrolytes (P series). P1 and P3 samples using HMDI have higher conductivity than P2 and P4 samples using the TDI in the backbone of PEUA. On the other hand, P5 with more PC content has higher conductivity than that of P6. This result shows that the effect of PC for reducing the crystallinity and for lowering T_g was very important.

The temperature dependency of ionic conductivity for polymer electrolytes is usually analyzed by the Vogel–

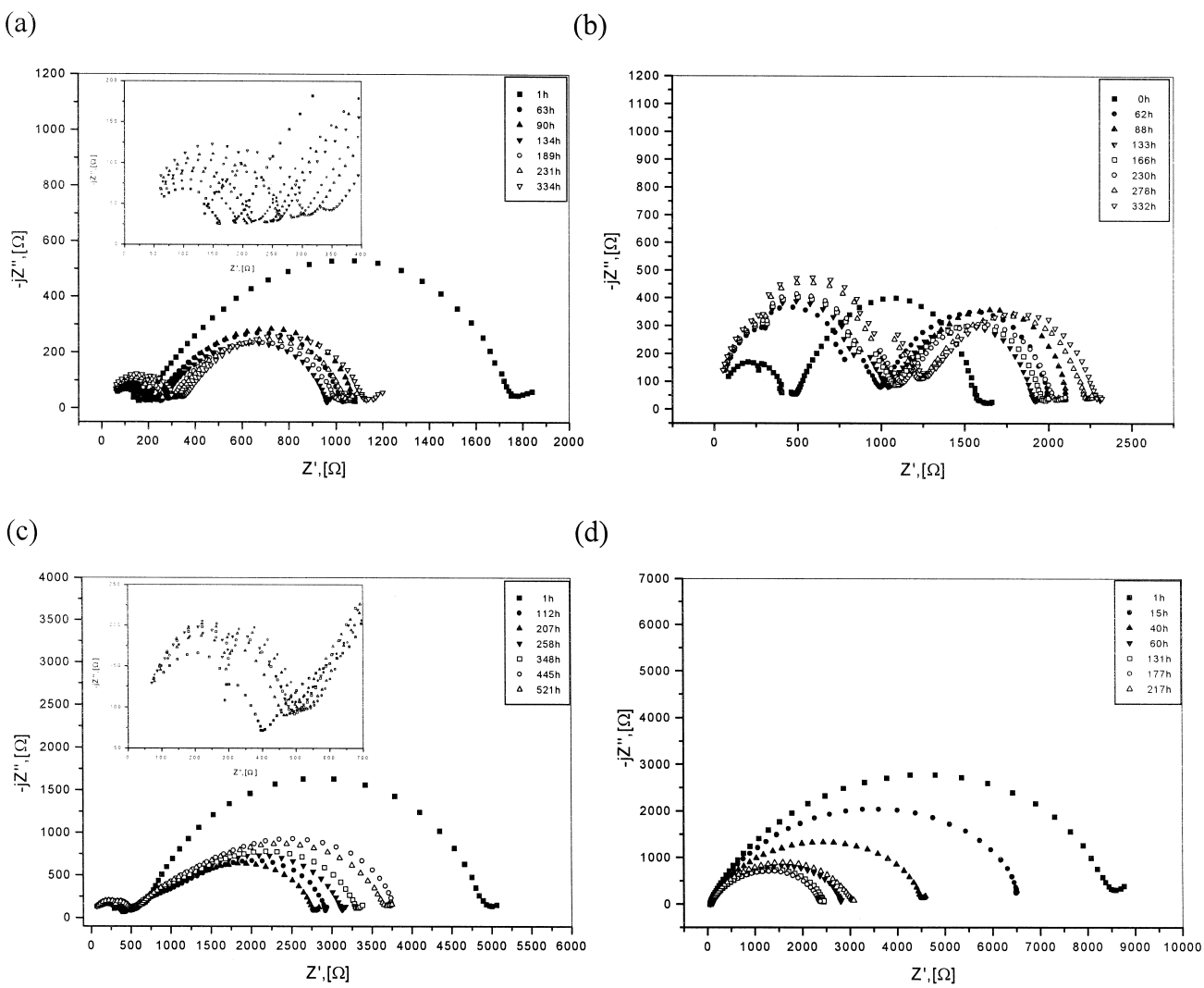

Fig. 7. Time evolution of the impedance of (a) P1 (PEG 200 10/HMDI 20/FA2D 20/PC 78.11/$LiCF_3SO_3$ 11.89), P2 (PEG 200 10/TDI 20/FA2D 20/PC 78.11/$LiCF_3SO_3$ 11.89), P3 (PEG 400 10/HMDI 20/FA2D 20/PC 75.84/$LiCF_3SO_3$ 14.16) and P5 (PPG1000 5/HMDI 10/FA2D 10/PC 85.55/$LiCF_3SO_3$ 9.48). Lithium cell stored under open circuit condition at 25°C. The number of progressive hours of storage is indicated in the figure.

Tammann–Fulcher (VTF) phenomenological relationship. It is well accepted that the variation of the conductivity with temperature for the majority of completely amorphous polymer electrolyte systems departs from the classical Arrhenius relationship [14]. Generally speaking, the VTF equation holds for solid polymer electrolyte at higher temperatures and for gel-type polymer electrolyte and it represents the coupling between ionic transport and polymer segmental motion. The VTF equation is an empirical equation that was originally formulated to describe the properties of supercooled liquids [14–17];

$$\sigma(T) = A_\sigma T^{-1/2} \exp\left[-\frac{E_a}{k_B}/(T - T_0)\right] \quad (3)$$

Here, A_σ is a constant related to the number of charge carrier, E_a is the pseudo-activation energy related to polymer segmental motion, and T_0 is the temperature at which the configurational entropy of the polymer becomes zero

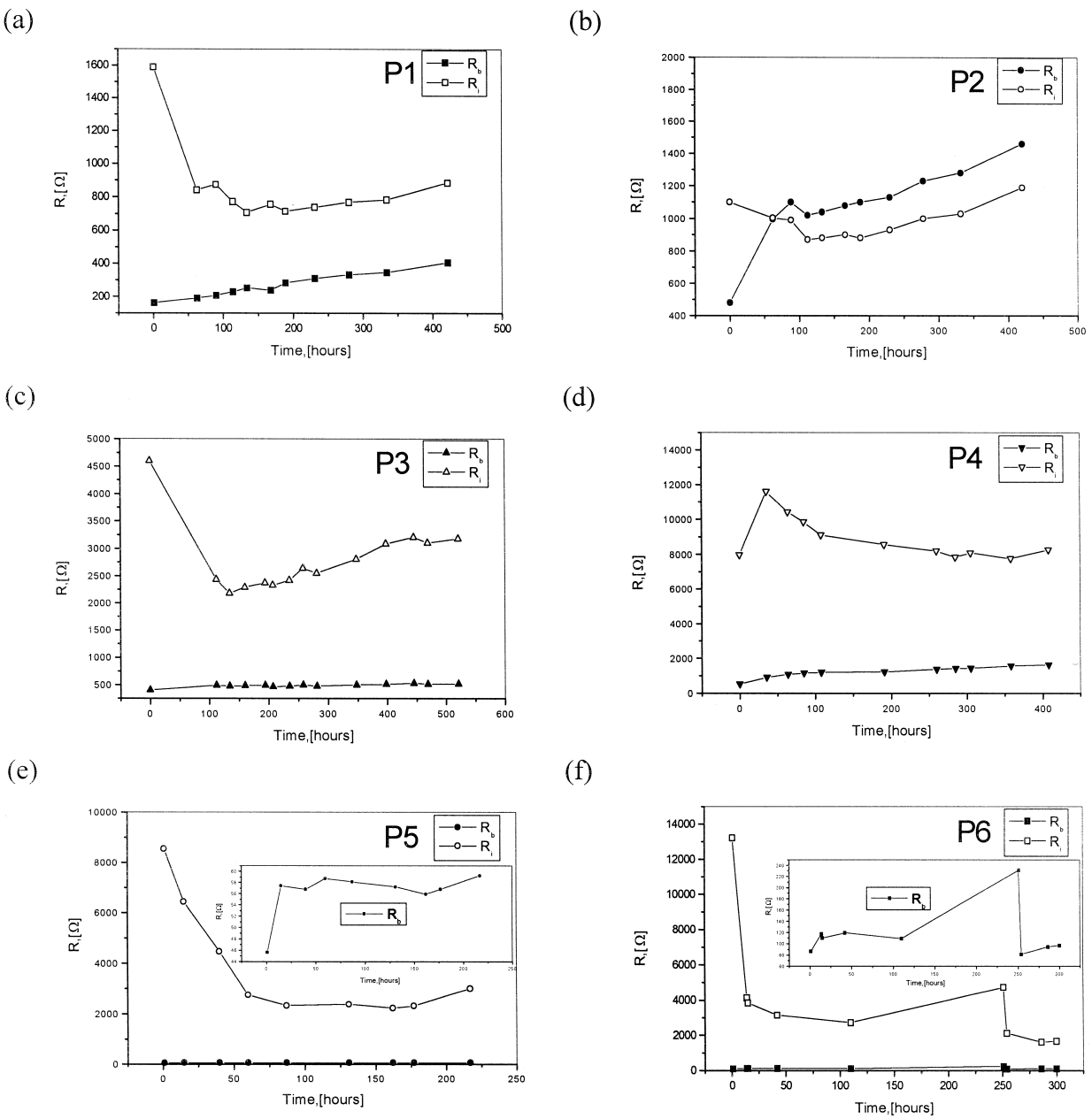

Fig. 8. Time evolution of the bulk resistance R_b and of the interfacial resistance R_i of the lithium electrode (a) in P1 (PEG 200 10/HMDI 20/FA2D 20/PC 78.11/$LiCF_3SO_3$ 11.89), (b) in P2 (PEG 200 10/TDI 20/FA2D 20/PC 78.11/$LiCF_3SO_3$ 11.89), (c) in P3 (PEG 400 10/HMDI 20/FA2D 20/PC 75.84/$LiCF_3SO_3$ 14.16), (d) in P4 (PEG 400 10/TDI 20/FA2D 20/PC 75.84/$LiCF_3SO_3$ 14.16), (e) in P5 (PPG1000 5/HMDI 10/FA2D 10/PC 85.55/$LiCF_3SO_3$ 9.48) and (f) P6 (PPG2000 5/HMDI 10/FA2D 10/PC 81.47/$LiCF_3SO_3$ 13.53).

and is usually associated with the ideal glass transition temperature (T_g) at which free volume disappears. However the T_0 values are anomalous and do not show the expected decrease or increase in the glass transition temperature with PC content and with modification of the PEUA backbone.

In the host PEUA matrix without the PC plasticizer, since the host PEUA matrix is relatively immobile, the long range transport of lithium cations must involve dissociation steps where solvated lithium cations are transferred between neighboring coordination sites in combination with migration and diffusion of ionic aggregates weakly coordinated to the polymer host. When the PC plasticizer was added in the host PEUA matrix, it modified the host PEUA matrix by lowering the crystallinity, and the viscosity and increased the ionic motion by reducing the potential barrier to ionic motion. Also, the PC plasticizer with high dielectric constant augmented the dissociation of $LiCF_3SO_3$, thereby increased the number of charge carriers and consequently ionic conductivity.

Since the electrochemical properties of the PEUA–$LiCF_3SO_3$-based polymer electrolytes were influenced by modifications of the PEUA backbone, we suggest that lithium cations are complexed with both polar sites (–O–, –NH–, –COO–) in the PEUA polymer network and the PC solvent, while the anions normally occupy voids in the system instead of being coordinated to polar sites in the host matrix even if solvated by PC. But the structures of plasticized PEUA polymer electrolytes have not been well understood. The fitted VTF parameters are summarized in Table 3. The highest conductivity is found for P5 using PPG1000 and HMDI. The conductivity of P5 is 3.1×10^{-4} S cm^{-1} at 25°C. The conductivities of other samples at 25°C are summarized in Table 4.

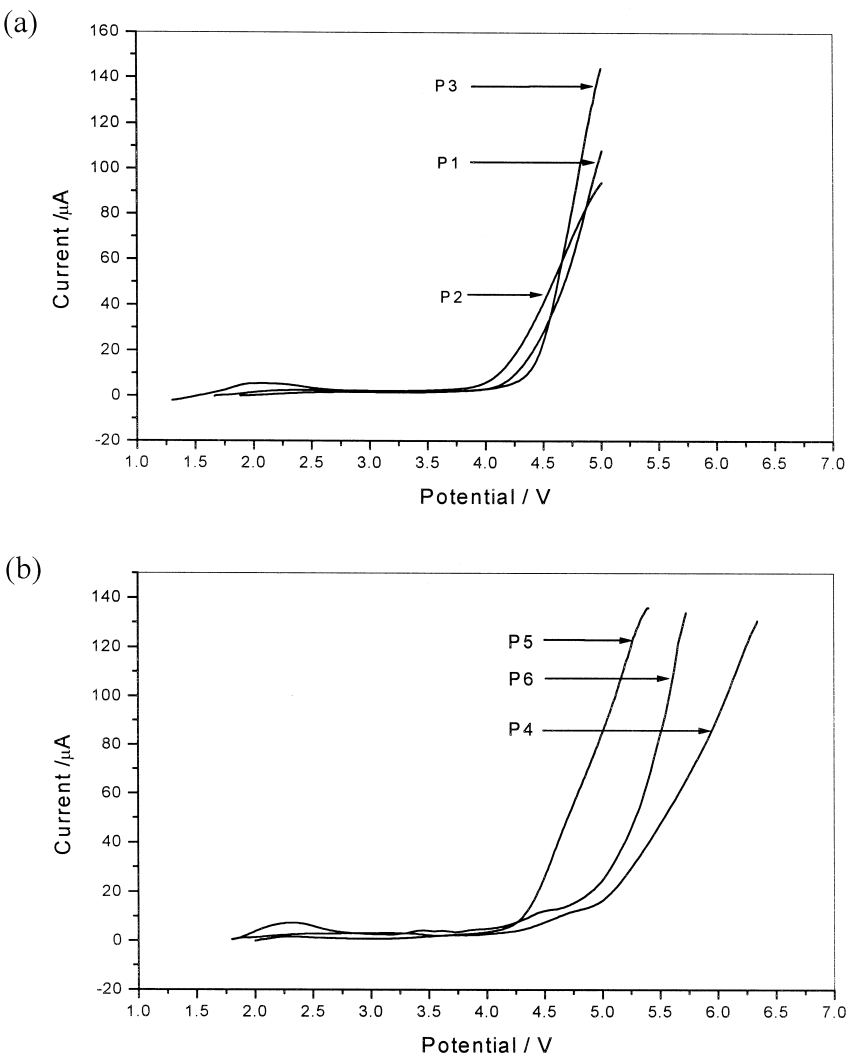

Fig. 9. Current–voltage curves of Li/PEUA polymer electrolyte/SS cells for (a) P1 (PEG 200 10/HMDI 20/FA2D 20/PC 78.11/$LiCF_3SO_3$ 11.89), P2 (PEG 200 10/TDI 20/FA2D 20/PC 78.11/$LiCF_3SO_3$ 11.89), and P3 (PEG 400 10/HMDI 20/FA2D 20/PC 75.84/$LiCF_3SO_3$ 14.16) and for (b) P4 (PEG 400 10/TDI 20/FA2D 20/PC 75.84/$LiCF_3SO_3$ 14.16), P5 (PPG1000 5/HMDI 10/FA2D 10/PC 85.55/$LiCF_3SO_3$ 9.48), and P6 (PPG2000 5/HMDI 10/FA2D 10/PC 81.47/$LiCF_3SO_3$ 13.53) at 25°C. Sweep rate: 1 mV/s. SS = stainless steel (SS 304). Electrolyte surface: 1.77 cm^2.

3.3.2. Compatibility

Compatibility with the electrode material is an essential parameter in the cyclability and the reliability of lithium battery. To determine the stability of the lithium–PEUA polymer electrolyte interface, we have carried out an impedance analysis of symmetrical Li/PEUA polymer electrolyte/Li cells stored and tested under open circuit conditions at room temperature. Fig. 7 illustrates the results obtained with four of six P samples which have a good electrochemical properties. In Fig. 7(a), (b) and (c) consist of two distorted semicircles. The high-frequency semicircles for different times of storage appeared to be a superposition of two semicircles having different time constants. We suspect that this profile is based on the microstructure of the sample. Similar profiles have been reported for the polymer complexes formed by segmented polyether poly(urethane urea) and lithium perchlorate by Watanabe et al. [18]. The favorable properties of polyether poly(urethane urea) (PEUU) as thermoplastic elastormers are based on their distinct two-phase microstructure. Also like PEUU, PEUA have the structure $(A–B)_n$, where A is a polyether segment (soft segment), B is an isocyanate part of polymer (hard segment). At a given temperature, the soft segment is in the rubbery state, whereas the hard segment is in the glassy or semicrystalline state. The hard segmental domains operate as hard fillers.

In Fig. 7, the $-jZ''–Z'$ plot reveals a progressive expansion of the middle frequency semicircle. The effect in lithium cells may be typically attributed to interfacial phenomena [6]. In fact, the expansion of the semicircle may be associated with a continuous growth of a resistive layer on the lithium electrode surface and indicates that lithium electrode is passivated in contact with the PEUA–$LiCF_3SO_3$-based polymer electrolytes. The structure of this layer is not known but it is very important parameter because such uncontrolled passivation phenomena affect the cyclability of lithium electrodes and therefore the entire lithium battery. In Fig. 7, the expansion of the semicircles and the growth of the resistive layer do not follow a regular trend.

Fig. 8 shows the time evolution of the bulk resistance and interfacial resistance. Although no clear explanation may be provided at this time, one can tentatively associate the fluctuations in the bulk resistance observed for the P

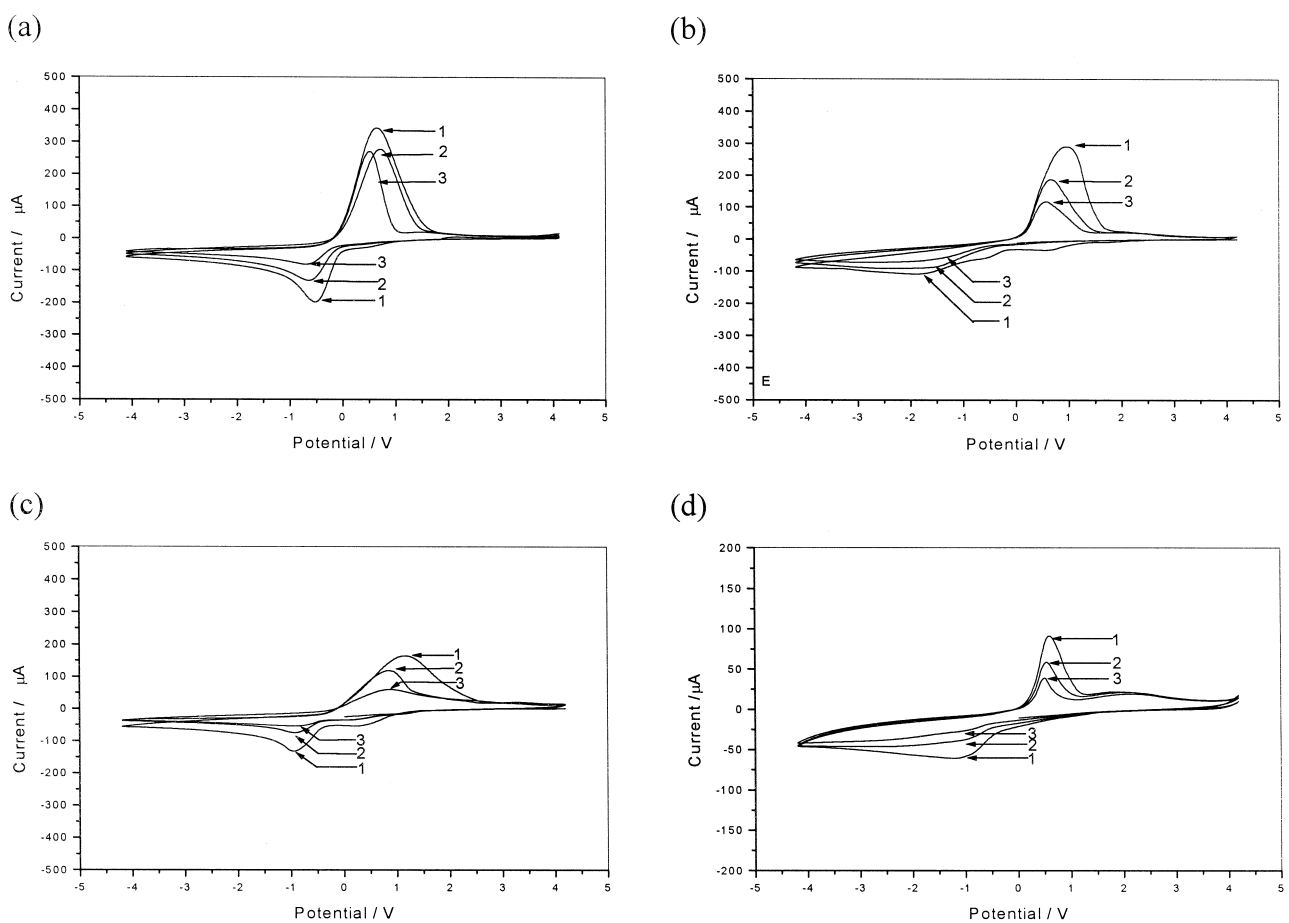

Fig. 10. Cyclic voltammograms of the lithium deposition–stripping process from (a) P1 (PEG 200 10/HMDI 20/FA2D 20/PC 78.11/$LiCF_3SO_3$ 11.89), (b) P3 (PEG 400 10/HMDI 20/FA2D 20/PC 75.84/$LiCF_3SO_3$ 14.16), (c) P4 (PEG 400 10/TDI 20/FA2D 20/PC 75.84/$LiCF_3SO_3$ 14.16), (d) P5 (PPG1000 5/HMDI 10/FA2D 10/PC 85.55/$LiCF_3SO_3$ 9.48) electrolyte on a stainless-steel substrate. Lithium counter and reference electrode at 25°C. Scan rate: 1 mV s^{-1}. The scan number is reported for each curve.

samples with changes in the actual content of the solvent, due to evaporation, reaction with lithium, etc. Similar results have been obtained with cells using other PEUA polymer electrolytes. In the PAN-based gel electrolytes [5], the passivation layer grows continuously and shows a cumulative trend which becomes dramatic with storage time. On the contrary, PEUA-based polymer electrolytes do not show such a dramatic effect.

4. Cyclic votammetry

4.1. Electrochemical stability window

Fig. 9 shows sweep voltammetry curves of cells formed by sandwiching a given PEUA–$LiCF_3SO_3$-based polymer electrolytes between two stainless steel blocking electrodes. As it is well known, the onset of current flow in this type of cell may be associated with the decomposition voltage of the given electrolyte [19]. The trend of the curve of Fig. 9 provides the evaluation of the anodic electrochemical stability of the PEUA polymer electrolytes. The stability of the electrolytes is influenced partially by the choice of the backbone of PEUA since it has the range of 4.0–4.8 V vs. Li at 25°C. The electrochemical stabilities of PEUA–$LiCF_3SO_3$-based polymer electrolytes (4.0–4.8 V) were slightly lower than PAN-based (4.3–5.0 V) [5] or PMMA-based gel electrolytes (4.5–4.8 V) [6].

4.2. Kinetics of the lithium deposition–stripping process

The kinetics of the lithium deposition–stripping process in the two electrodes was studied. Fig. 10 shows the cyclic voltammograms of the lithium deposition–stripping process from samples used in this study, respectively. The potential limits were imposed by ± 4.2 V for testing a useful stability range. A single anodic stripping peak follows a single cathode deposition peak. This suggests that the PEUA–$LiCF_3SO_3$-based polymer electrolytes chosen were stable [8]. As electrolyte reacted with lithium electrode and formed passive film, the lithium stripping peak decreased [6].

5. Lithium transference number

In Table 4 the electrochemical properties of the PEUA–$LiCF_3SO_3$-based polymer electrolytes show that conductivity, the lithium ion transference number, and decomposition voltage of electrolytes depend on modifications of the backbone of PEUA. Lithium ion transference number values obtained for the six samples were between 0.5 and 0.3. PEUA–$LiCF_3SO_3$-based polymer electrolytes (0.3–0.5) have lower transference number than PAN-based (0.6–0.8) [5] or PMMA-based gel electrolytes (0.5–0.7) [6].

6. Conclusions

The PEUA–$LiCF_3SO_3$-based polymer electrolytes were synthesized by fast UV-curing. Conductivity in PEUA–$LiCF_3SO_3$-based polymer electrolytes was influenced by the structure of PEUA in some degree and by a plasticizing solvent PC mostly. Samples using HMDI had higher conductivity than samples using the TDI in the backbone of PEUA. The addition of a plasticizing solvent PC to a PEUA–$LiCF_3SO_3$-based polymer electrolytes modified the electrolytes by reducing the crystallinity and by lowering T_g and viscosity. This consequently increases the mobility of all articles by reducing the potential barrier to ionic motion. P5 (PPG1000 5/HMDI 10/FA2D 10/PC 85.55/$LiCF_3SO_3$ 9.48) with the most PC content of six PEUA–$LiCF_3SO_3$-based polymer electrolytes had the highest conductivity which was 3.1×10^{-4} S cm^{-1} at 25°C. Compatibility between the PEUA–$LiCF_3SO_3$-based polymer electrolyte film and the lithium metal electrode was not very good because a passive film was formed on the lithium electrode by reaction between the electrolyte and lithium. The passivation layer of the PAN-based gel electrolytes grows continuously and shows a cumulative trend which becomes dramatic with storage time [5], on the contrary, PEUA-based polymer electrolytes do not show such a dramatic effect because the hard segmental domains operate as hard fillers. But it was not fully understood how PEUA–$LiCF_3SO_3$-based polymer electrolytes would render the interface with lithium metal more stable. Decomposition voltage of PEUA was 4.0–4.8 V vs. Li. Since it depends on concentrations and sorts of the salt and solvents, etc., decomposition voltage may be extended to higher voltage. Transference numbers were 0.3–0.5. Although PEUA had lower transference number than that of the PAN-based or PMMA-based gel electrolyte, this value was not poor and the same as that of nonaqueous liquid electrolytes. PEUA–$LiCF_3SO_3$-based polymer electrolytes had a slightly lower electrochemical value than PAN-or PMMA-based polymer electrolytes partly. But PEUA–$LiCF_3SO_3$-based polymer electrolytes are good candidates for the lithium batteries because they has also considerable merit in mechanical and electrochemical properties.

References

[1] J.H. Lai, in: J.S. Tonge, D.F. Shriver (Eds.), Polymers for Electronic Applications, CRC Press, Boca Raton, FL, 1989, p. 158.
[2] B. Scrosati, Nature 373 (1995) 557.
[3] M. Alamgir, K.M. Abraham, J. Power Sources 54 (1995) 40.
[4] D. Baril, C. Michot, M. Armand, Solid State Ionics 94 (1997) 35.
[5] F. Croce, F. Gerace, G. Dautzemberg, S. Passerini, G.B. Appetecchi, B. Scrosati, Electrochim. Acta 39 (1994) 2187.
[6] G.B. Appetecchi, F. Croce, B. Scrosati, Electrochim. Acta 40 (1995) 991.
[7] W. Wieczorek, J.R. Stevens, J. Phys. Chem. B 101 (1997) 1529.
[8] J.F. Le Nest, A. Gandini, H. Cheradame, Br. Polymer J. 20 (1998) 253.

[9] M.C. Borghini, M. Mastragostino, A. Zanelli, Electrochim. Acta 41 (1996) 2369.
[10] S. Velankar, J. Pazos, S.L. Cooper, J. Appl. Polym. Sci. 62 (1996) 1361.
[11] N.S. Allen, M.S. Johnson, P.K.T. Oldring, S. Salim, in: P.K.T. Oldring (Ed.), Chemistry and Technology of UV and EB Formulations for Coatings, Inks and Paints, Vol. 2, SITA, London, UK, 1991, p. 115.
[12] P.G. Bruce, C.A. Vincent, J. Electroanal. Chem. 225 (1987) 1.
[13] M. Watanabe, K. Sanui, N. Ogata, T. Kobayashi, Z. Ohtaki, J. Appl. Phys. 57 (1985) 123.
[14] F.M. Gray, in: J.A. Connor (Ed.), Polymer Electrolytes, School of Chemistry, Univ. of St. Andrews, UK, 1997, p. 113.
[15] H. Vogel, Z. Phys. 22 (1921) 645.
[16] Fulcher, J. Am. Chem. Soc. 8 (1925) 339.
[17] G. Tamman, W. Hesse, Z. Anorg. Allg. Chem. 156 (1926) 245.
[18] M. Watanabe, S. Oohashi, K. Sanui, N. Ogata, T. Kobayashi, Z. Ohtaki, J. Macromolecules 18 (1985) 1945.
[19] G.B. Appetecchi, G. Dautzenberg, B. Scrosati, J. Electrochem. Soc. 143 (1996) 6.